Measurements of Film Flow Rate in Heated Tubes with Various Axial Power Distributions

by

Carl Adamsson

February 2006
Technical Reports from
Royal Institute of Technology
KTH Nuclear Reactor Technology
SE-106 91 Stockholm, Sweden

Akademisk avhandling som med tillstånd av Kungliga Tekniska Högskolan i Stockholm framlägges till offentlig granskning för avläggande av teknologie licentiatexamen måndagen den 13 Mars 2006 kl 10.15 i Seminarierum 112:028, Reaktorteknologi, Alba Nova, Roslagtullsbacken 11, Stockholm.

Universitetsservice US–AB, Stockholm 2006

Carl Adamsson 2006, **Measurements of Film Flow Rate in Heated Tubes with Various Axial Power Distributions**

KTH Nuclear Reactor Technology, SE-106 91 Stockholm, Sweden

Abstract

Measurements of film mass flow rate for annular, diabatic steam-water flow in tubes are presented. The measurements were carried out with four axial power distributions and at several axial positions at conditions typical for boiling water reactors, i.e. 7 MPa pressure and total mass flux in a range from 750 to 1750 kg/m^2s. The results show that the influence of the axial power distribution on the dryout power corresponds to a consistent tendency in the film flow rate and that the film tends to zero when dryout is approached. Furthermore it is demonstrated that two selected phenomenological models of annular flow well predict the present data. A model for additional entrainment due to boiling is shown to degrade the predictions.

Descriptors: film flow, film thickness, dryout, power distribution, annular flow

Preface

This thesis consists of two parts. The first is an introduction and summary of the present work that provides some background and overview as well as summarizes the main results and conclusions. The second part consists of three published papers, which have been adjusted to comply with the format of the thesis, but have not been changed except for minor refinements.

December 2005, Stockholm
Carl Adamsson

Contents

Part I

Overview and summary

CHAPTER 1

Introduction

1.1. Background

In many boiling systems, and in particular in water cooled nuclear reactors, the maximal possible power is limited by a phenomenon called critical heat flux (CHF). It appears as a sudden detoriation of the heat transfer process when the power exceeds a certain limit, which causes a sharp rise in the heater temperature that is likely to destroy the heater. It is obvious that measures must be taken to prevent CHF from occurring, either by limiting the power or by optimizing the construction in order to increase the margins to CHF. In either case accurate methods to predict the phenomenon are needed.

The CHF phenomenon is not easy to define in general terms, but if the discussion is limited to steady-state heat flux controlled systems, the following definition will be satisfactory:

> The critical heat flux is the heat flux at which further increase of the power will result in a sudden increase of the heater temperature.

This definition is based on how the CHF phenomenon is usually measured and not on the underlying mechanism that caused it. In fact, there are several different mechanisms that may give rise to a rapid wall temperature increase. Thus, the definition above does not really refer to one phenomenon but rather to a whole class of related phenomena, which will occur in many types of boiling systems. This thesis, however, is concerned only with the type of CHF that typically occurs in boiling water nuclear reactors (BWR) and is usually termed dryout. In pressurized water reactors (PWR) another phenomenon occurs that fits the CHF definition given above. It is usually called departure from nucleate boiling (DNB) and the mechanism is different from that of dryout. The DNB phenomenon will not be further considered in this thesis. It is just noted here that DNB typically occurs when the bulk liquid is subcooled through the formation of a thin vapor film at the heated surface. Dryout, on the other hand, is associated with the annular flow regime. That is, the vapor phase forms the core of the flow while the liquid travels partly as a liquid film on the walls and partly as drops entrained in the vapor. Dryout occurs when the liquid film is no longer able to wet the wall.

A large amount of work, over several decades, has been spent on understanding how the dryout phenomenon arises. Today the fundamental mechanisms are, at least qualitatively, well understood, but some questions remain open. It is generally agreed upon that dryout occurs when the liquid film is no longer able to efficiently wet the wall so that heat, instead of evaporating the film, must be transported away from the wall by significantly less efficient forced convection to vapor. It is also clear that deposition of entrained drops to the film and mechanical entrainment of film into drops are highly crucial mechanisms. What is less clear is whether the film thickness will go continuously to zero as the dryout power is approached or if there is a critical film thickness where the film, for one reason or another, will suddenly break up and dryout occur. Experiments by Milashenko *et al.* (1989) and Ueda & Isayama (1981) indicate significant critical film thickness, while experiments by Hewitt *et al.* (1965) and, as will be shown, the present experiments imply that it is negligible. This discrepancy is most likely due to the fact that the first two experiments, which showed critical film, were performed in much shorter tubes (around 1 m) and correspondingly higher heat fluxes than the latter. This only confirms that dryout changes into a different phenomenon (DNB) at low steam quality.

Another interesting and not fully settled question is that of the role of the heat flux (apart from the obvious effect as the source of evaporation). It has sometimes been treated as the main parameter controlling the CHF phenomenon, which is evident from the name critical heat flux itself as well as from the traditional way of constructing dryout correlations (see chapter 3.1). Experiments by Groeneveld (1975) with a 'flux spike', however, showed that at low steam quality the onset of CHF indeed follows the local heat flux but at high steam quality the the spike had almost no effect with the mean flux instead controlling the dryout. Again this confirms that CHF is different at low respective high steam quality but also shows that the use of the local heat flux in dryout models is not straight forward. It has been argued that the rate of entrainment depends strongly on the heat flux (Milashenko *et al.* 1989), while other models have been constructed with no such influence at all (Hewitt & Govan 1990). Yet other models have mixed the two approaches, see e.g. Hoyer (1998) and Okawa *et al.* (2003).

The discussion in the previous paragraph leads directly to that of the influence of the power distribution. For it is so that, even if the local heat flux is not directly controlling the dryout phenomenon, neither is the mean heat flux along the channel enough. On the contrary it is well known that shifting the power towards the outlet, where the steam quality is high, will decrease the dryout power, while shifting it towards the inlet will increase the power at which dryout occurs. (See e.g. Blomstrand *et al.* (2000))

The mechanism behind this behavior was qualitatively explained by an elegant series of experiments by Bennett *et al.* (1966). They measured the film

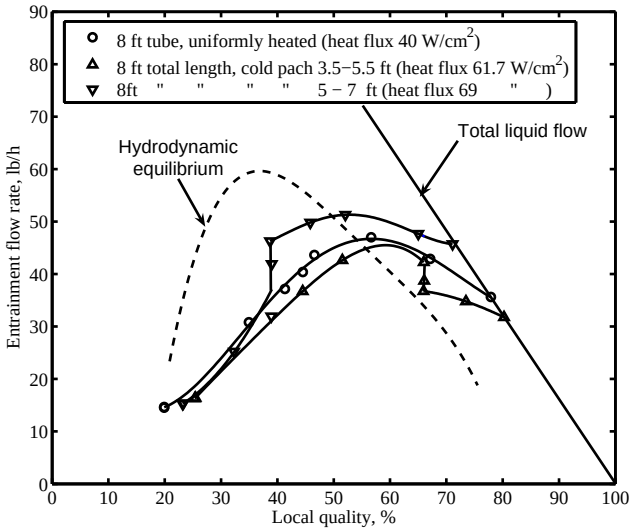

FIGURE 1.1. Reproduced from Bennett *et al.* (1966)

flow rate in a heated pipe, where the power profile contained moveable cold patches. Strikingly it was possible to achieve higher dryout power with a cold patch close to the outlet than with a completely uniform power distribution.

The mechanism is most readily explained with help of Figure 1.1 that is reproduced from the original paper. The figure shows the flow rate of entrained drops against the steam quality for different placements of the cold patch together with the hydrodynamic equilibrium curve (from measurements in very long adiabatic pipes). At the cold patches the entrained drop curve tends towards the equilibrium curve. When the cold patch is close to the inlet this leads to an increased drop flow rate and thus a reduction in the dryout steam quality. When the cold patch is close to the outlet, on the other hand, the tendency towards equilibrium will reduce the amount of drops and increase the dryout steam quality. Dryout is here supposed to occur when the entrained drop curve meets the total liquid line, i.e. when the film flow rate is zero.

1.2. Objectives

The objective of the present work is primarily to confirm the findings by Bennett *et al.* (1966) for several realistic power distributions at conditions typically found in a BWR and to extend the database of film measurements that can be used for direct validation of phenomenological models of annular two-phase flow.

To study the phenomena of deposition and entrainment it is almost necessary to have information about axial development of the liquid film. This means that a single measurement of the film close to the channel exit is not enough. The present experimental program therefore includes measurements at several axial positions for each power distribution.

Since the high-pressure two-phase loop was not equipped with the measurement system needed for this type of experiments, it had to be constructed (see Chapter 2). In order to simplify the necessary installations and to be able to study one pure physical effect, the experiments were carried out in the simplest possible geometry, i.e. a round tube without any spacer grids or other obstacles. The influence of the power distribution is rather weak in such a system compared to more complex geometrical configurations with spacer grids, but the simplicity of the measurement system and the analysis that could be achieved nevertheless made this choice preferable.

CHAPTER 2

Experimental Techniques

2.1. Earlier Experiments

Since dryout is triggered by the disappearance of the liquid film from the heated surface, the key to understanding the phenomenon is accurate measurements of the film. For this purpose one could measure either the thickness of the film or the film mass flow rate. The thickness has been measured with needle probes (Würtz 1978) and conductance probes (Collier & Hewitt 1964). These techniques are fast and make it possible to measure not only the average film thickness but also the waves traveling with the film. In dryout modeling, however, it is usually the mass flow rate that turns up in the equations, since this parameter can easily be related to the mass- and energy balances. For that reason it was decided to measure the film mass flow rate in this project.

A technique to do that by extracting the liquid film through the wall of the test-section has been shown to be reliable by several studies before. The idea is to slowly increase the extraction rate from a low value and at each step measure the amounts of liquid and gas in the sample. (In air-water systems this can be done with a separator, for steam-water systems the most reliable method is to condense the sample and rely on the heat balance as described below). When the flow of liquid no longer increases as the extraction rate is increased, it is assumed that the film flow rate has been found.

The earliest such experiments were performed on air-water systems and a slit in the wall was used to extract the film (Bennett & Thornton 1961). Since large waves in the film tend to overshoot the slit, it was replaced by a porous wall section in later studies. Hewitt *et al.* (1965) and Hewitt & Pulling (1969) used sinter metal wall sections and Würtz (1978) used a 5 cm wall section perforated with 1.2 mm holes. Singh *et al.* (1969) studied the influence of the length of the porous wall section and concluded that waves will overshoot if it is too short. On the other hand, if it is too long the measurements will be inaccurate. It was recommended to use a length of 1 in. In accordance with this recommendation, the present study used a 30 mm sinter metal wall section (with effective length slightly shorter).

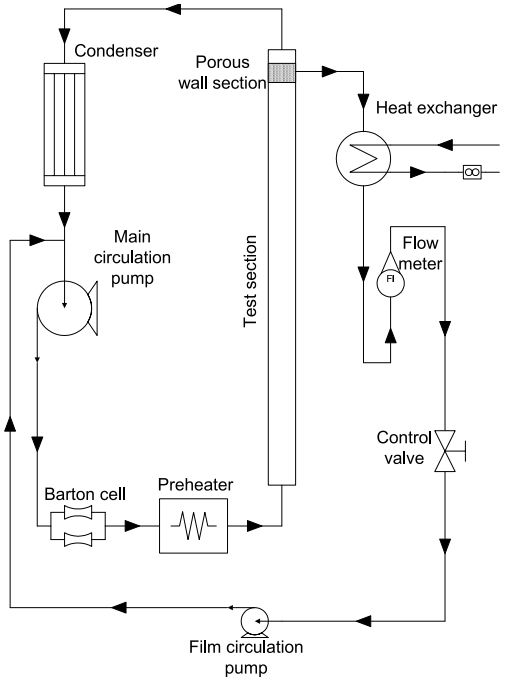

FIGURE 2.1. Working principles of the main loop and the film extraction loop.

2.2. Present Experimental Setup

The working principle of the main loop and the film measurement system is shown in Figure 2.1. Before the test-section, the water passed through a 150 kW preheater to achieve the desired inlet temperature. The test-sections were manufactured from 3.65 m long stainless steel pipes with 14 mm inner diameter and were heated by an electric current (DC) in the steel. The power was calculated as the product of this current and the voltage over the test-section and the power distribution was imposed by letting the outer diameter of the pipe vary (thereby varying the electrical resistance).

The power distributions that were studied in the present work are shown in Figure 2.2 and Table 1 in Appendix A. (The power distributions shown are the actual power distributions obtained by measuring the local electrical resistance of the test-sections). These four distributions – the uniform, inlet peaked, middle peaked and outlet peaked – were chosen to be able to study the well documented effect of decreasing dryout power when the power peak

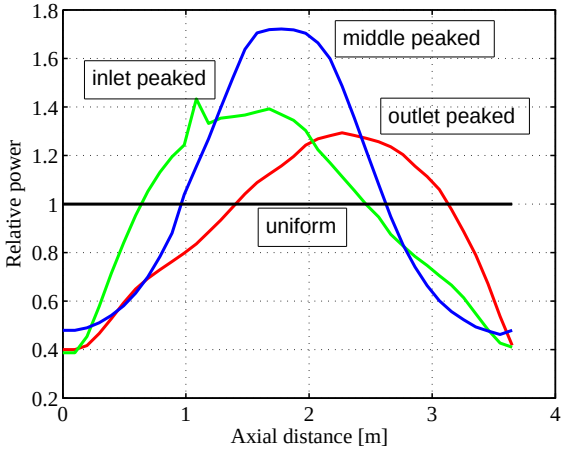

FIGURE 2.2. The four axial power distributions used in the experiments. The spike in the inlet peaked distribution is a manufacturing fault.

moves towards the exit and since a large amount of dryout data are available for these distributions.

The water was then condensed before it passed through the main circulation pump and the flow measurement system, which consisted of four 1000 mm long pipes with various diameters. The flow rate measurements were based on measuring the pressure drop over one of these pipes with a Barton cell.

To this was added the film extraction loop with a heat exchanger, flow meter and a second circulation pump. The purpose of the heat exchanger was to condense the extracted sample before it entered the flow mater. The vapor content could then be calculated by monitoring the temperatures and flow rates at the primary and secondary sides of the heat exchanger. These calculations, which were carried out automatically by a LABVIEW software during the measurements, are described in detail in Paper 3.

The results were analyzed graphically by plotting the extracted liquid flow rate against the vapor fraction in the sample to obtain an L-shaped curve as shown in Figure 2.5. The film flow rate could be read off as the intersection of the vertical part of the curve with the horizontal axis. (For details about the analysis of the extraction curves and more examples, see Paper 1 and Paper 3).

Figures 2.3 and 2.4 show photographs of the film extraction device and the sinter metal section that was used in the experiments. Note the small distance between the power clamp to the right in Figure 2.3 and the extraction point. It

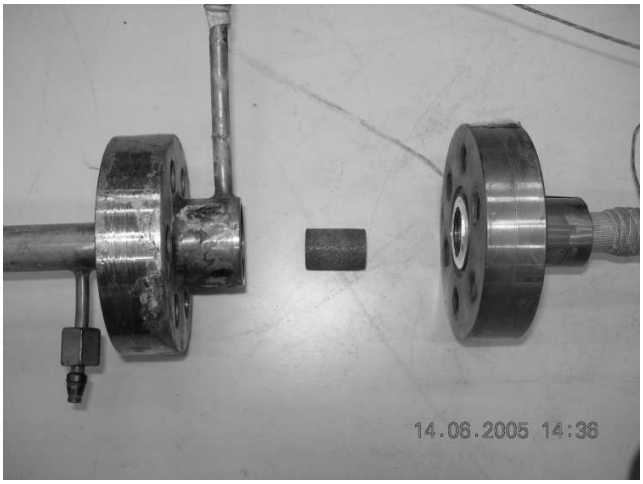

FIGURE 2.3. Side view of dismounted film extraction device.

FIGURE 2.4. The porous sinter metal part mounted in the film extraction device.

is important to have this distance as small as possible to prevent redeposition of drops before the measurement point.

The heat exchanger was placed as close as possible to the extraction point and was well insulated to prevent heat losses in the connection pipe. Several thermocouples were used to measure the various temperatures at the primary

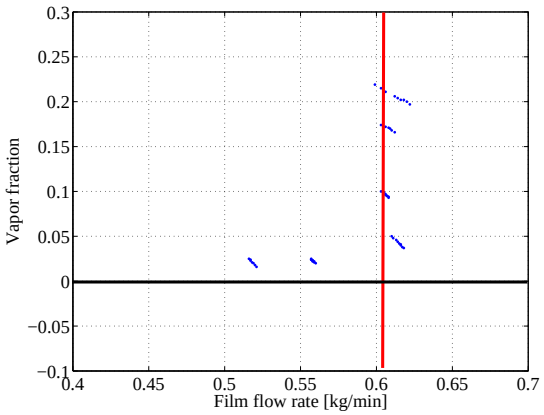

FIGURE 2.5. Example of suction curve from the experiments. The film flow rate is determined from the intersection of the vertical part of the curve with the horizontal axis.

and secondary sides. This redundancy in the temperature measurements made it easier to estimate the accuracy (see Chapter 2.4).

2.3. Measurement Procedure

For each experiment the first step was to establish steady-state in the main loop at the desired conditions. The sample flow rate through the porous wall was then adjusted to a low value (compared to the expected film flow rate). After a couple of minutes a steady-state had developed in the main loop and the heat exchanger in the film extraction loop. (The LABVIEW software used had functions to help the operators maintain the steady-state during the measurements). All monitored parameters of the system were then saved, the sample flow rate was increased and a new steady-state was allowed establish itself. This continued until as much as possible of the expected L-shaped curve was obtained, which could usually be accomplished within half an hour.

The use of stainless steel implied that the test-section could not withstand post-dryout conditions (other options were considered but ruled out for practical reasons). Hence all experiments had to be performed with some margin to the dryout condition. The procedure used was to start each series of measurements by finding the dryout power at the corresponding flow rate. The steam quality was then reduced by approximately 3% and the film flow measurements started from that lower power. A second series of measurements was also carried out at approximately 10% reduced power. (The full matrix of experiments can be found in Paper 3).

For the uniform power distribution the effective axial position of the filter was changed by changing the inlet temperature, thereby moving the onset of

boiling without changing the heat flux. This procedure is however not possible for the non-uniform distributions. In these cases the test-sections had to be dismounted, cut and reassembled again.

After this operation the power to the test-section must be adjusted to reproduce the local heat flux (as opposed to the mean). To achieve this, the local heat flux was measured by monitoring the voltage over a short section of the test-section close to the inlet. The local power could then be calculated as the product of this voltage and the current in the test-section.

2.4. Accuracy

The accuracy of the results from measurements is naturally an issue of major importance. The errors that will always be present in any experimental data can be divided in two types – random uncertainties and systematic errors. The random part is caused by the uncertainty of the instrumentation and can relatively easily be analyzed. The systematic errors are due to possible physical effects that were not considered in the analysis of the data. Examples that should be considered are heat losses in the equipment, consequences of waves on the film surface and redepositon of entrained drops before the extraction point.

A thorough analysis of both the random uncertainties and systematic errors can be found in Paper 3. It was concluded that the main source of uncertainties was the flow measurements in the film loop. In the present project a rotameter from KROHNE was used for this purpose. It was calibrated to be accurate within 2% for flow rates between 0.3 and 3.0 kg/min. When the measured film flow rate was small this accuracy was not fully satisfactory and at the end of the project the equipment was complemented with an addition flow meter of turbine type, calibrated for low flow rates. It proved to be more reliable than the rotameter and it is hence recommended to replace the rotameter with a turbine flow meter in future measurements.

It was also concluded in Paper 3 that heat losses in the extraction loop and redeposition of drops were small enough to be neglected. The interpretation of the suction curves, however, sometimes constitutes a significant error source. More examples of exctraction curves can be found in Paper 1 and Paper 3 and it is clear from the figures there that not all the curves had the ideal L-shape shown in Figure 2.5. Sometimes the deviation could be explained by disturbance waves on the film surface, but in other cases it must be treated as an uncertainty of the measurement equipment. (See Paper 3 for examples and a more detailed discussion of this issue).

Finally it was estimated that measurements with reasonably sharp and readily interpreted suction curves could be considered to be accurate within ± 0.1 kg/min and measurements with distorted suction curves were considered

accurate within ± 0.2 kg/min. All error bars shown in this thesis are based on that estimate.

CHAPTER 3

Models and Correlations

3.1. Dryout Correlations

Even though a lot of work has been done to formulate accurate models of the dryout phenomenon, the method that is most commonly used in practice is empirical correlations (or lookup tables). In this section the theoretical basis for such methods is outlined in order to conclude when they should be used and when they can be expected to fail.

The system analyzed here is a general, vertical channel of any geometry (tube, annulus, rod bundle or other) with upwards flowing boiling water and heat applied through one or more walls. Furthermore it is assumed that the system operates under steady-state conditions. The discussions will also be limited to the case when the inlet is subcooled for reasons explained below.

Now define a set of parameters – or boundary conditions – that can be assumed to completely define the state of the system for a fixed geometry. The state here refers to all aspects of the system in which we have any interest, in particular whether any part of the heated surface is in dryout or not. One such set of boundary conditions consists of:

- inlet mass flux (G)
- inlet enthalpy (h_{in})
- outlet pressure (p)
- average heat flux ($\overline{q''}$)
- channel length (L)

Note that these parameters are easily defined in terms of single numbers. The reason to assume a subcooled inlet is that if a two-phase mixture were introduced at the inlet the conditions there would have to be specified in more detail.

There is one additional parameter – the power distribution. It can be defined as a function that to each part of the wetted wall assigns a relative heat flux, i.e. the ratio of the local heat flux to the average heat flux. The power distribution can obviously not be described with a single number. With the assumption that the five parameters above (assuming constant, but not necessarely uniform power distribution) completely define the state of the system and given a large enough matrix of dryout experiments on this geometry it is

possible to construct a four dimensional lookup-table of the critical heat flux or, alternatively, to fit a mathematical function in four variables to the data.

Considering the physics it is, however, possible to introduce additional simplifying assumptions. Since the inlet is subcooled there will be single-phase flow in the lowest part of the channel. In this part it may be assumed that the conditions are completely described by the mass flux and the fluid enthalpy. (Note that this would not be true for phenomena such as DNB or subcooled boiling, but here only dryout at high steam quality is considered). With this assumption a new (artificial) inlet could be defined anywhere in the subcooled region and in particular at the onset of boiling, where the enthalpy can be assumed to be that of saturation at the given pressure and thus be omitted as a boundary condition.

In this way the defining set is reduced to:

- inlet mass flux (G)
- outlet pressure (p)
- average heat flux ($\overline{q''}$)
- boiling length (L_b)

From these parameters the (equilibrium) outlet steam quality may be calculated and, if so prefered, replace any one of the parameters in the defining set. Replacing the boiling length with the outlet steam quality gives the classical heat flux/steam quality correlation form (see Hewitt in Hetsroni (1982)). Note that it is the average heat flux and outlet steam quality that appears in the correlation as it was derived here, not the local values. Replacing the heat flux in the defining set with the steam quality gives another classical correlation form: the steam quality/boiling length. It is clear from the argument here that the two forms are completely equivalent. That is, as long as the power profile is kept constant (but not necessarily uniform), which is a fundamental assumption for the reasoning in this chapter and thus the weakness of all dryout correlations.

Thus it can be concluded that empirical correlations can be expected to work if only a limited number of parameters, which are possible to describe with single numbers, are varied and enough data for calibration are available. When parameters are varied that can not be described with single numbers, such as the geometry or the power distribution, the correlation concept will most possibly fail. In such cases, and when there are not enough data to calibrate a correlation properly, models built on physical reasoning must be considered.

3.2. Phenomenological Models

Many models of annular flow with the aim to predict the dryout power have been formulated. Most of them are built on the assumption that annular flow in one dimension can be described as a vapor core with entrained liquid drops and a liquid film on the wall and that three main mass transfer mechanism are

working: evaporation of film into vapor, deposition of drops that become film and entrainment of film into drops. The simplest models are based only on the mass conservation for the liquid film, which can be written as:

$$\frac{1}{P}\frac{dW_f}{dz} = D - E - \Gamma \tag{3.1}$$

where W_f denotes the liquid film flow rate, P is the wall perimeter and D, E and Γ are the deposition rate, entrainment rate and evaporation rate respectively. The evaporation rate can easily be calculated from the wall heat flux, but for the deposition and entrainment processes, empirical or semi-empirical correlations are usually used.

Equation 3.1 must be equipped with an appropriate boundary condition. Since the equation can be expected to describe the flow only when the flow regime is annular, it is natural to impose the boundary condition at the beginning of annular flow. Thus, in addition to models for the deposition and entrainment rates a model for the onset of annular flow and the film flow rate there is necessary. For very long channels (more than 6–7 m) the boundary condition is not particularly important, but in the present case it is of crucial importance for the model.

3.3. Deposition Models

Most models for the deposition of drops to the walls are based on the assumption that the phenomenon is caused by a diffusion like mechanism. It is then natural to assume that the deposition rate should be related to the concentration of drops in the vapor core. It is therefore common to introduce a deposition velocity, k_d, as:

$$D = k_d C \tag{3.2}$$

where C is the effective drop density in the vapor core. A large number of empirical correlations for k_d have been published. Hewitt & Govan (1990) proposed the following expression:

$$k_d = 0.083 \max\left(0.3, \frac{C}{\rho_v}\right)^{-0.65} \sqrt{\frac{\sigma}{\rho_v d_h}} \tag{3.3}$$

which was modified by Okawa *et al.* (2003) to read

$$k_d = 0.0632 \left(\frac{C}{\rho_v}\right)^{-0.5} \sqrt{\frac{\sigma}{\rho_v d_h}} \tag{3.4}$$

Other correlations are, for example, due to Sugawara (1990), de Bertodano & Assad (1998) and Utsuno & Kaminaga (1998).

3.4. Entrainment Models

For entrainment models the diversity is larger. Since the entrainment rate is very difficult to measure, the only data that is available is for hydrodynamic equilibrium, where $D = E$, so that the entrainment rate is given by the deposition correlation. Many entrainment correlations are therefore return-to-equilibrium models, based on the assumption $E = k_d C_{eq}$, where the effective drop concentration at equilibrium, C_{eq}, is correlated. With this approach it is, however, easy to get unphysical models, since correlations for C_{eq} are usually not given in the relevant local parameters.

The entrainment process is highly complex and all details are not well understood, but there are correlations with more physically plausible form than the simple return-to-equilibrium. For example, Hewitt & Govan (1990), proposed

$$E = 5.75 \cdot 10^{-5} \left(\left(G_f - G_{f,crit} \right)^2 \frac{d_h \rho_l}{\sigma \rho_v^2} \right)^{0.316} G_v \tag{3.5}$$

where G denotes mass flux, ρ density, σ surface tension and d_h is the hydraulic diameter of the channel. Indices v, l and f refer to the vapor phase, liquid phase and film, respectively. $G_{f,crit}$ is given by a separate correlation and denotes the onset of entrainment, i.e. the film flow rate below which no entrainment occurs.

The inventors of this correlation did not give any detailed motivation for its form, but it is written in terms of hydrodynamically relevant local parameters, such as the vapor mass flux and local film mass flux. (With some minor modifications equation 3.5 can be written in terms of the film wall flux, W_f/P, which is the physically relevant parameter if several films are present in the channel).

Okawa *et al.* (2003) presented an entrainment rate correlation based on dimensional reasoning and the hypothesis that the entrainment rate is primarily governed by the shear stress acting on the film (see also Okawa *et al.* (2002)). The authors gave the correlation in terms of the superficial velocities of film and vapor as:

$$E = k_e \rho_l \frac{f_i \rho_v J_v^2 \delta}{\sigma} \left(\frac{\rho_l}{\rho_v} \right)^n \tag{3.6}$$

$$\delta = \frac{1}{4} \sqrt{\frac{f_w \rho_l}{f_i \rho_v}} \frac{J_f}{J_v} d_h \tag{3.7}$$

where $k_e = 4.79 \cdot 10^{-4}$ m/s, $n = 0.111$ and f_i and f_w are the interfacial and wall friction factors respectively (definitions are not repeated here). Here J denotes the superficial velocity and δ models the film thickness.

Equation 3.6 can be rearranged into a form rather similar to equation 3.5 above. It then becomes:

$$E = k_e \frac{S f_i}{\sigma} \frac{d_h G_f}{4} \left(\frac{\rho_l}{\rho_v} \right)^n G_v \tag{3.8}$$

$$S = \sqrt{\frac{f_w \rho_l}{f_i \rho_v}} \tag{3.9}$$

where S is a model of the slip ratio.

In the same paper it was proposed that to this shear induced entrainment add a term for entrainment due to boiling, based on a correlation originally developed by Ueda *et al.* (1981) for falling liquid films. As was briefly discussed in Chapter 1, such heat flux induced phenomena are probably important in short channels with high heat flux, but when compared with the present data, the agreement was better without this term (see Paper 2).

A slightly different form of the correlation 3.6 was shown to be able to capture the influence of the axial power distribution on the dryout power in Okawa *et al.* (2004). This feature, and that the correlation is based on physical reasoning, made it interesting for comparison with data from the present project.

3.5. Models for the Boundary Condition

As mentioned above, the boundary condition at the onset of annular flow can be crucial for the success of the model if the channel is not very long. At the same time, this boundary condition is probably the most uncertain part of phenomenological dryout modeling, primarily because film flow measurements in this region are very difficult.

To close equation 3.1 it is necessary to specify the film flow rate at the beginning of annular flow as well as a model for where the transition to annular flow occurs. Unfortunately, correlations for deposition and entrainment are sometimes given without this informatin, which makes them difficult to apply in practice.

A common assumption is that deposition and entrainment are in equilibrium at the beginning of annular flow. This assumption was successfully used by Okawa *et al.* (2003), who used a correlation for the transition to annular flow and calculated film flow rate by setting the deposition and entrainment correlations equal at that point. Hewitt & Govan (1990) mention the assumption of 99% of the liquid to be entrained as drops at a quality of 0.1, but also that their results were insensitive to this assumption. Since this boundary condition would not reproduced the data presented here, the boundary condition given by Okawa *et al.* (2003) was used instead.

CHAPTER 4

Summary of Results

4.1. Critical Film Thickness

As was mentioned in Chapter 1 it is not fully clear whether the film flow rate goes continuously to zero when dryout is approached or if it suddenly breaks up at some positive critical film thickness. The measurements on the uniform power distribution are particularly useful to investigate this, by slightly extrapolating the results to the power where dryout was measured. (No measurements could be performed at dryout conditions for practical reasons). Such an investigation was presented in Paper 1 and it was concluded that for the investigated conditions the critical film thickness would, within the accuracy of the measurements, for practical purposes be negligible.

This conclusions is in agreement with measurements with similar conditions performed by Hewitt *et al.* (1965). Measurements in much shorter pipes (around 1 m) by e.g. Milashenko *et al.* (1989) and Ueda & Isayama (1981), however, have shown significant critical film thickness, indicating that the results of the present measurements are not valid for high enough heat fluxes.

4.2. Influence of the Power Distribution

In Chapter 1 the explanations by Bennett *et al.* (1966) of the influence of the power distribution were recapitulated. Their conclusion was that the effect is hydrodynamical and results in more entrained drops at the exit of the pipe if the power is shifted towards the outlet (in their case by introducing a cold patch close to the inlet).

The main purpose of the present project was to confirm these conclusions for realistic power distributions that can be found in a typical BWR. One difficulty was that the difference between the power distributions is rather small in tubes without spacers grids, see Figure 4.1. (It is much larger in complex geometries, such as rod bundles, that are always equipped with spacer grids). Thus, to see the effect the accuracy of the measurements must be quite high. Nevertheless, in Paper 3 it was demonstrated that the present measurements can resolve the difference between the inlet peaked and outlet peaked distributions and that the tendency in the entrained drop flow rate is consistent with the conclusions by Bennett *et al.* (1966). That is, there is more

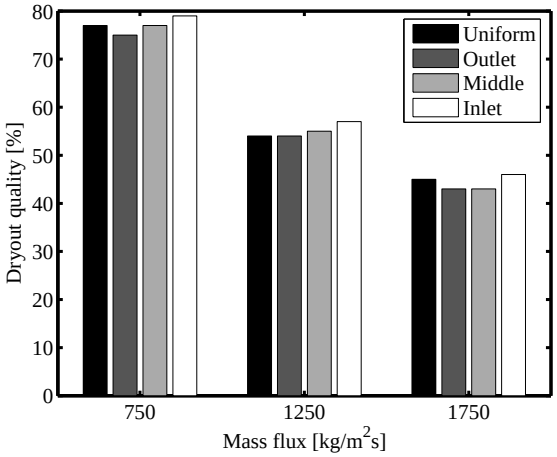

FIGURE 4.1. Dryout steam quality for the investigated conditions; four axial power distributions and three flow rates.

entrained drops and thus less film when the power distribution is outlet peaked. The results of the current measurements are illustrated in Figure 4.2.

As can also be seen in the figure it was difficult to conclude much for the middle peaked distribution, since the results were similar (within the accuracy of the measurements) to what was obtained for the inlet peaked profile.

4.3. Comparison with Models

Obviously, the measurements presented here should be compared with existing phenomenological models of annular flow and dryout. Two models, due to Hewitt & Govan (1990) and Okawa *et al.* (2003), were selected for this purpose. Both models use semi-empirical correlations, which have been tuned against measurements of film flow and dryout power, to describe the deposition and entrainment processes. One difference is that the second model contains a term that depends on the local heat flux and is supposed to model entrainment due to nucleate boiling within the liquid film (see Chapter 3.2).

In Paper 2 these two models were compared with the present measurements of the uniform and outlet peaked power distributions. It was concluded that both models were in excellent agreements with the measurements provided that the boiling entrainment term was removed from the second model. This result indicates that boiling entrainment is not a significant effect at the investigated conditions.

The comparison in Paper 2 was carried out by using one measurement point as boundary condition for the models, thus avoiding the problem of modeling the boundary condition. Paper 3 presented comparisons with the same two

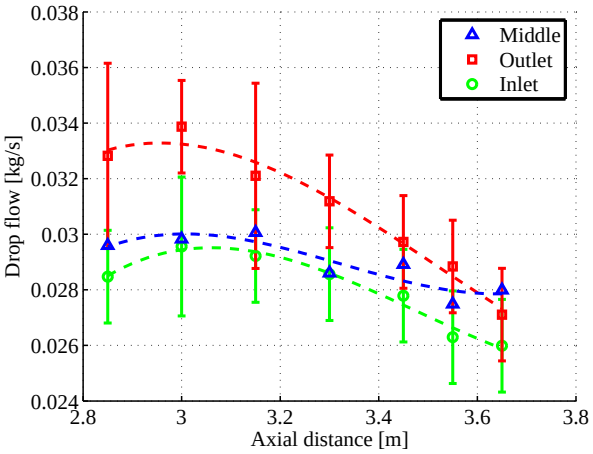

FIGURE 4.2. Drop flow versus axial distance for inlet-, middle- and outlet-peaked axial power distributions. Mean heat flux 0.74 MW/m^2, total mass flux 750 kg/m^{2}s, pressure 70 bar, inlet subcooling 10 K.

models but with the boundary condition proposed in the paper by Okawa *et al.* (2003). Again the agreement between models and measurements was excellent, but it is evident from Figure 4.3 that the largest difference between the models occur in the lower part of the channel where no measurements were available.

An intersesting observation, not included in any of the papers, is shown in Figures 4.4(a) and 4.4(b). As can be seen, the model by Okawa *et al.* (2003) correctly predicts the tendency of more entrained drops for the outlet peaked power distribution, but the model by Hewitt & Govan (1990) does not. One would then expect the latter model would also fail to predict the trend in dryout power, but this does not happen. The reason is that the erroneous trend seen in Figure 4.4(b) reverses when the power is increased and film flow approaches zero.

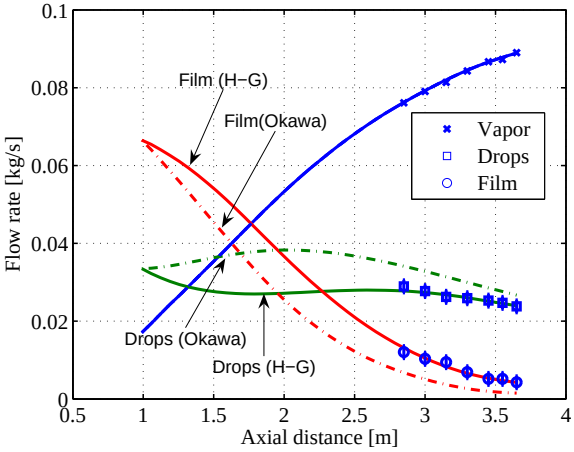

FIGURE 4.3. Comparison of measured flow rates with predictions by Hewitt & Govan (1990) and Okawa *et al.* (2003) models. Inlet-peaked axial power distribution, mean heat flux 0.86 MW/m^2, mass flux 1750 kg/m^{2}s, pressure 7 MPa and inlet subcooling 10 K.

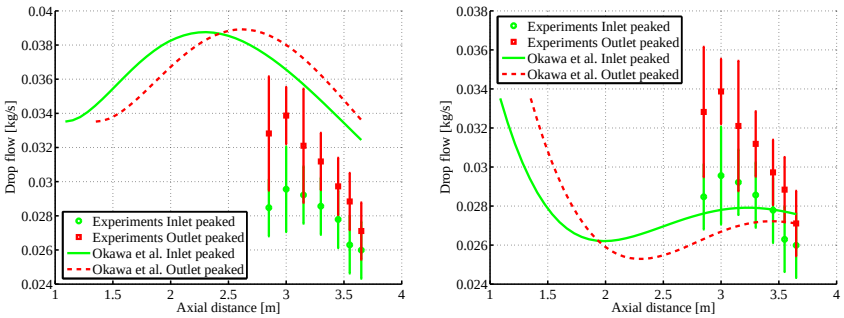

(a) Okawa *et al.* (2003) (b) Hewitt & Govan (1990)

FIGURE 4.4. Flow rate of entrained drops at mass flux 750 kg/m^{2}s and mean heat flux 0.74MW/m^2, according to experiments and two phenomenological models.

CHAPTER 5

Conclusions and Future Work

In this thesis measurements of the film flow rate in heated round tubes have been presented. The results show that the axial power distribution has an influence on the drop flow rate and thereby on the film flow rate and that this influence is consistent with the well known tendency in the dryout power. These results are consistent with other available data with simpler power distributions. The conclusion is that the hydrodynamical explanation of this effect is at least qualitatively correct also for power distributions and thermodynamic conditions typically found in a boiling water nuclear reactor.

It has also been shown that the film flow rate tends to zero (within the accuracy of the measurements) when the dryout power is approached. Hence no critical film model should be necessary for the heat flux and flow conditions considered here. Also this conclusion is consistent with earlier measurements at similar conditions.

Since the measurements presented here were carried out at several axial positions for each set of boundary conditions, they are well suited for comparison with phenomenological models of annular flow. The comparison that has been presented here shows that two selected phenomenological models well reproduce the experimental data. The largest discrepancy between the two models, however, occurred in the lower part of the channel where no measurements were available.

There are many ways this work could be extended and continued. If better accuracy could be achieved, a more detailed comparison of more power profiles would be possible. The simplest way to improve the accuracy is most probably to replace the flow meter in the extraction loop with a more accurate instrument. It might also be possible to improve the temperature measurements on the secondary side of the heat exchanger. Distorted extraction curves are more difficult to remedy, but having eliminated other error sources it might be possible to correct them for the effects of large disturbance waves.

The parameter range covered by the present project was very limited. It would be of interest to extend it, primarily to higher flow rates but also to vary the pressure and inlet temperature. The measurements would probably be more difficult at high flow rates, though (because of low steam quality and thus thick films a large amounts of entrained drops that can disturb the measurements).

It is also likely that capacity of the heat exchanger and flow meter must be extended to be able to handle higher flow rates.

Finally, it would be of interest to investigate the influence of spacer grids on the liquid film. Measurements of the dryout power show that spacer grids, depending on their design, can significantly increase the dryout power. Models for this effect exist, but there is not much detailed film flow data available for validation. With one moveable spacer close to the exit of the pipe, this effect could be investigated with the present equipment. It is also likely that one or more spacer grids in the pipe would increase the difference between the power distributions, thereby making a comparison between them easier.

Acknowledgements

First of all I would like to thank my supervisor Prof. Henryk Anglart for all support during the work and for interesting discussions, comments and criticism.

Stellan Hedberg cannot be thanked enough for making this project possible with his technical skills and knowledge, for constructing the equipment, repairing it when it broke down and for spending many hours in the lab with me during the measurements and error searching.

Thanks also to my co-supervisor Per Person for sharing his experience, the LABVIEW code for the main loop and for showing a lot of interest in the project.

The Swedish Center for Nuclear Technology (SKC) is gratefully acknowledged for their financial support and Westinghouse Electric Company for giving me the opportunity to do this. My reference group has contributed with valuable comments and generally showed interest in the project, which is appreciated.

Finally I would like to thank my colleagues and friends at KTH for creating a pleasant and creative working environment.

References

Bennett, A. & Thornton, I. 1961 Data on vertical flow of air-water mixtures in the annular and dispersed flow regions. part i: Preliminary study. *Trans. Inst. Chem. Engrs.* **39**, 101–112.

Bennett, A. W., Hewitt, G. F., Kearsey, H., Keeys, R. & Pulling, D. 1966 Studies of burnout in boiling heat transfer to water in round tubes with non-uniform heating. *Tech. Rep.* R5076. AERE.

de Bertodano, M. L. & Assad, A. 1998 Entrainment Rate of Droplets in the Ripple-Annular Regime for Small Vertical Ducts. *Nuclear Science and Engineering* **129**, 72–80.

Blomstrand, J., Behamin, D., Persson, P. & Hedberg, S. 2000 Loop studies simulating – in annular geometry – the influence of the axial power distribution and the number of spacers in 8x8 bwr assemblies. In *2nd Japanese-European Two-Phase Flow Group Meeting*.

Collier, J. G. & Hewitt, G. F. 1964 Film thickness measurement. *ASME paper 64–WA/HT–41* .

Groeneveld, D. 1975 The effect of short flux spikes on the dryout power. *Tech. Rep.* AECL–4927. Atomic Energy of Canada Ltd.

Hetsroni, G., ed. 1982 *Handbook of Multiphase Systems*. Hemisphere Publisher Corporation.

Hewitt, G. & Govan, A. 1990 Phenomenological modeling of non-equilibrium flows with phase change. *Int. J. Heat and Mass Transfer* **33** (2), 229–242.

Hewitt, G., Kearsey, H., Lacey, P. & Pulling, D. 1965 Burnout and film flow in the evaporation of water in tubes. *Tech. Rep.* R4864. AERE.

Hewitt, G. & Pulling, D. 1969 Liquid entrainment in adiabatic steam-water flow. *Tech. Rep.* R5374. AERE.

Hoyer, N. 1998 Calculation of dryout and post–dryout heat transfer for tube geometry. *International Journal of Multiphase Flow* **24** (2), 319–334.

Milashenko, V., Nigmatulin, B., Petukhov, V. & Trubkin, N. 1989 Burnout and distribution of liquid in evaporative channels of various lenghts. *International Journal of Multiphase Flow* **15** (3), 393–401.

Okawa, T., Kitahara, T., Yoshida, K., Matsumoto, T. & Kataoka, I. 2002 New entrainment rate correlation in annular two-phase flow applicable to wide

range of flow conditions. *International Journal of Heat and Mass Transfer* **45**, 87–98.

Okawa, T., Kotani, A., Kataoka, I. & Naito, M. 2003 Prediction of Critical Heat Flux in Annular Flow Using a Film Flow Model. *Journal of Nuclear Science and Technology* **40** (6), 388–396.

Okawa, T., Kotani, A., Kataoka, I. & Naito, M. 2004 Prediction of critical heat flux in annular regime in various vertical channels. *Nuclear Engineering and Design* **229**, 223–236.

Singh, K., Pierre, C., Crago, W. & Moeck, E. 1969 Liquid Film Flow-Rate in Two-Phase Flow of Steam and Water at 1000Lb/Sq.In.Abs. *AIChE Journal* **15** (1).

Sugawara, S. 1990 Droplet deposition and entrainment modeling based on the three-fluid model. *Nuclear Engineering and Design* **122** (67).

Ueda, T., Inoue, M. & Nagatome, N. 1981 Critical heat flux and droplet entrainment rate in boiling of falling liquid films. *International Journal of Heat and Mass Transfer* **24** (7), 1257–1266.

Ueda, T. & Isayama, Y. 1981 Critical heat flux and exit film flow rate in flow boiling system. *International Journal of Heat and Mass Transfer* **24** (7), 1267–1276.

Utsuno, H. & Kaminaga, F. 1998 Prediction of Liquid Film Dryout in Two-Phase Annular-Mist Flow in a Uniformly Heated Narrow Tube. Development of Analytical Method under BWR Conditions. *Journal of Nuclear Science and Technology* **35** (9), 643–653.

Würtz, J. 1978 An Experimental and Theoretical Investigation of Annular Steam-Water Flow in Tube and Annuli at 30 to 90 bar. *Tech. Rep.* 372. RisøNational Laboratory.

APPENDIX A

Power profiles

TABLE 1. Relative power for the four axial power distributions as function of the axial coordinate. The values were obtained by resistance measurements of the test-section. There is a spike in the inlet peaked profile due to a manufacturing fault.

z [m]	uni.	inl.	mid.	out
0.099	1.000	0.387	0.479	0.400
0.197	1.000	0.454	0.490	0.417
0.296	1.000	0.578	0.511	0.467
0.395	1.000	0.714	0.541	0.527
0.493	1.000	0.839	0.580	0.592
0.592	1.000	0.953	0.633	0.650
0.691	1.000	1.052	0.700	0.694
0.789	1.000	1.131	0.783	0.729
0.888	1.000	1.195	0.880	0.763
0.986	1.000	1.243	1.039	0.798
1.085	1.000	1.433	1.155	0.836
1.184	1.000	1.332	1.269	0.885
1.282	1.000	1.354	1.396	0.933
1.381	1.000	1.360	1.520	0.988
1.480	1.000	1.367	1.638	1.042
1.578	1.000	1.380	1.705	1.089
1.677	1.000	1.392	1.719	1.123
1.776	1.000	1.369	1.721	1.157
1.874	1.000	1.345	1.718	1.196
1.973	1.000	1.303	1.704	1.243
2.072	1.000	1.224	1.664	1.269
2.170	1.000	1.170	1.600	1.282
2.269	1.000	1.113	1.486	1.294
2.368	1.000	1.056	1.355	1.283
2.466	1.000	0.997	1.218	1.271
2.565	1.000	0.947	1.081	1.257
2.664	1.000	0.875	0.948	1.236
2.762	1.000	0.828	0.833	1.204
2.861	1.000	0.784	0.741	1.156
2.959	1.000	0.747	0.664	1.113
3.058	1.000	0.705	0.602	1.060
3.157	1.000	0.666	0.557	0.978
3.255	1.000	0.614	0.523	0.887
3.354	1.000	0.548	0.493	0.790
3.453	1.000	0.482	0.477	0.672
3.551	1.000	0.427	0.462	0.537
3.650	1.000	0.410	0.480	0.418